

Formation of a σ -alkane Complex and a Molecular Rearrangement in the Solid-State: $[\text{Rh}(\text{Cyp2PCH}_2\text{CH}_2\text{PCyp2})(\eta^2:\eta^2\text{-C}_7\text{H}_{12})][\text{BArF}_4]$

Citation for published version:

McKay, AI, Krämer, T, Rees, NH, Thompson, AL, Christensen, KE, Macgregor, SA & Weller, AS 2016, 'Formation of a σ -alkane Complex and a Molecular Rearrangement in the Solid-State: $[\text{Rh}(\text{Cyp2PCH}_2\text{CH}_2\text{PCyp2})(\eta^2:\eta^2\text{-C}_7\text{H}_{12})][\text{BArF}_4]$ ', *Organometallics*.
<https://doi.org/10.1021/acs.organomet.6b00645>

Digital Object Identifier (DOI):

[10.1021/acs.organomet.6b00645](https://doi.org/10.1021/acs.organomet.6b00645)

Link:

[Link to publication record in Heriot-Watt Research Portal](#)

Document Version:

Publisher's PDF, also known as Version of record

Published In:

Organometallics

General rights

Copyright for the publications made accessible via Heriot-Watt Research Portal is retained by the author(s) and / or other copyright owners and it is a condition of accessing these publications that users recognise and abide by the legal requirements associated with these rights.

Take down policy

Heriot-Watt University has made every reasonable effort to ensure that the content in Heriot-Watt Research Portal complies with UK legislation. If you believe that the public display of this file breaches copyright please contact open.access@hw.ac.uk providing details, and we will remove access to the work immediately and investigate your claim.

Formation of a σ -alkane Complex and a Molecular Rearrangement in the Solid-State: $[\text{Rh}(\text{Cyp}_2\text{PCH}_2\text{CH}_2\text{PCyp}_2)(\eta^2:\eta^2\text{-C}_7\text{H}_{12})][\text{BAr}^{\text{F}}_4]$

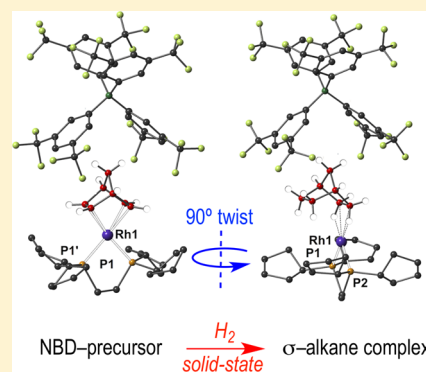
Alasdair I. McKay,^{†,§} Tobias Krämer,^{‡,§} Nicholas H. Rees,[†] Amber L. Thompson,[†] Kirsten E. Christensen,[†] Stuart A. Macgregor,^{*,‡} and Andrew S. Weller^{*,†}

[†]Department of Chemistry, University of Oxford, Mansfield Road, Oxford OX1 3TA, U.K.

[‡]Institute of Chemical Sciences, Heriot-Watt University, Edinburgh EH14 4AS, U.K.

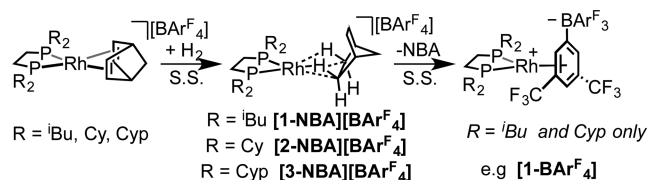
S Supporting Information

ABSTRACT: Addition of H_2 to the precursor $[\text{Rh}(\text{Cyp}_2\text{PCH}_2\text{CH}_2\text{PCyp}_2)(\eta^2:\eta^2\text{-C}_7\text{H}_8)][\text{BAr}^{\text{F}}_4]$ gives the σ -alkane complex $[\text{Rh}(\text{Cyp}_2\text{PCH}_2\text{CH}_2\text{PCyp}_2)(\eta^2:\eta^2\text{-C}_7\text{H}_{12})][\text{BAr}^{\text{F}}_4]$ by a single-crystal to single-crystal reaction, as characterized by X-ray crystallography, SSNMR spectroscopy, and periodic DFT. An unexpected rearrangement of the $\{\text{Rh}(\text{L}_2)\}^+$ fragment is revealed.



Complexes in which an alkane acts as a ligand to a metal center using its C–H bonding electrons, so-called σ -alkane complexes, are of considerable interest due to their role as intermediates in C–H activation processes and the challenges involved with their synthesis and characterization.¹ As C–H bonds are strong and non-nucleophilic, alkanes are very poor ligands, and direct observation of σ -alkane complexes has generally been limited to very low temperature in situ solution spectroscopic techniques.² We have recently reported that they may be prepared by solid/gas single-crystal to single-crystal transformations (Scheme 1),³ enabling structural

Scheme 1. Synthesis of σ -Alkane Complexes^a



^aS. S. = solid-state.

characterization by single crystal X-ray crystallography. Addition of H_2 to the diene precursor $[\text{Rh}(\text{R}_2\text{PCH}_2\text{CH}_2\text{PR}_2)(\eta^2:\eta^2\text{-NBD})][\text{BAr}^{\text{F}}_4]$ (NBD = norbornadiene, $\text{Ar}^{\text{F}} = 3,5\text{-(CF}_3)_2\text{C}_6\text{H}_3$) leads to the generation of $[\text{Rh}(\text{R}_2\text{PCH}_2\text{CH}_2\text{PR}_2)(\eta^2:\eta^2\text{-NBA})][\text{BAr}^{\text{F}}_4]$ (NBA = norbornane; R = *i*Bu, [1-NBA][BAr^F₄]; R = Cy, [2-NBA][BAr^F₄]). When R = *i*Bu, rapid loss of NBA in the solid-state at 298 K gives the [BAr^F₄]-coordinated zwitterion [1-BAr^F₄].⁴ In contrast, when R = Cy,

the σ -alkane complex is stable in the solid state for months at 298 K.⁵ The precise factors that are responsible for these differences are currently not fully resolved. Both species feature encapsulation of the cation by an octahedral arrangement of [BAr^F₄][−] anions, which provides a well-defined lattice environment, while the buttressing Cy groups in [2-NBA][BAr^F₄] may install a kinetic penalty toward rearrangement in the solid state.^{4,5} We now report the synthesis of $[\text{Rh}(\text{Cyp}_2\text{PCH}_2\text{CH}_2\text{PCyp}_2)(\eta^2:\eta^2\text{-NBA})][\text{BAr}^{\text{F}}_4]$ using a cyclopentyl (Cyp)-substituted chelating phosphine⁶ which was designed to sit between the steric profiles of flexible *i*Bu and rigid/tall Cy. This leads to not only a relatively stable σ -alkane complex but also an unexpected metal-fragment reorientation within the [BAr^F₄][−] anion cavity while retaining the integrity of the single crystal.

The precursor complex $[\text{Rh}(\text{Cyp}_2\text{PCH}_2\text{CH}_2\text{PCyp}_2)(\eta^2:\eta^2\text{-NBD})][\text{BAr}^{\text{F}}_4]$ ([3-NBD][BAr^F₄]) was prepared as for [2-NBD][BAr^F₄].⁵ A single-crystal X-ray diffraction study at 150 K⁷ (Figure 1A) demonstrated crystallographically imposed C₂ rotational symmetry with Rh1 and NBD bridge methylene (C7) occupying special positions. The Cyp groups are disordered, while the long-range structure was found to be modulated (Supporting Information),⁸ which was modeled with a *q* vector of (0,0.3433,0).⁹ The [BAr^F₄][−] anions are organized so that each cation is contained within a pseudo-octahedral cage of anions, and the overall motif and structural

Special Issue: Hydrocarbon Chemistry: Activation and Beyond

Received: August 11, 2016

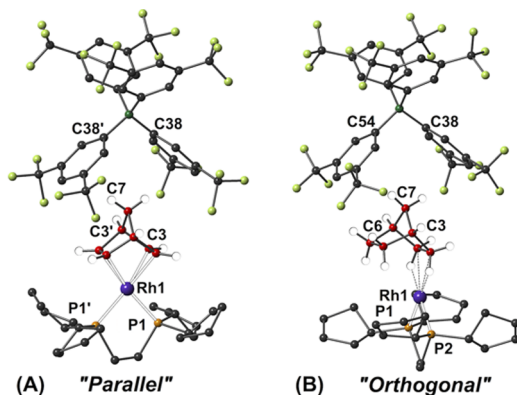


Figure 1. Solid-state structures (ball and stick) relative to a local $[\text{BARF}_4]^-$ anion: (A) $[\text{3-NBA}][\text{BARF}_4]$, average structure; (B) $[\text{3-NBD}][\text{BARF}_4]$. Selected interplane angles: $\text{C38}', \text{C38}, \text{Rh1}/\text{Rh1}, \text{P1}, \text{P1}' = 6.39(17)^\circ$; $\text{C38}, \text{C54}, \text{Rh1}/\text{Rh1}, \text{P1}, \text{P2} = 88.12(12)^\circ$.

metrics are very similar to those reported for $[\text{2-NBD}][\text{BARF}_4]$. In particular the NBD ligand sits in a cleft between two $[\text{BARF}_4]^-$ aryl groups so that the C7-methylene protons point toward the centers of two of the aromatic rings. In the 298 K $^{31}\text{P}\{\text{H}\}$ solid-state NMR (SSNMR) spectrum two distinct, but very close, phosphine environments are observed (δ 66.2, J_{RhP} 149 Hz; δ 65.7, J_{RhP} 151 Hz), consistent with PCyp₂ disorder and/or the modulated structure. In the $^{13}\text{C}\{\text{H}\}$ SSNMR spectrum four signals observed between δ 90 and 55 are assigned to the NBD fragment under C_2 symmetry. The disorder/modulation was not resolved in this spectrum.

Addition of H_2 to a single-crystal sample of $[\text{3-NBD}][\text{BARF}_4]$ (2 bar, 10 min, 298 K) led to the quantitative formation of the σ -alkane complex $[\text{Rh}(\text{Cyp}_2\text{PCH}_2\text{CH}_2\text{PCyp}_2)(\eta^2\text{-}\eta^2\text{-NBA})][\text{BARF}_4]$ ($[\text{3-NBA}][\text{BARF}_4]$) (Scheme 1). Crystallinity is retained in this process, and the resulting structure determined by single-crystal X-ray diffraction (100 K, $R(2\sigma) = 7.0\%$) clearly shows a saturated NBA fragment interacting with the Rh center through two 3c-2e $\text{Rh}\cdots\text{H}-\text{C}$ interactions, in which the relevant hydrogen atoms were located but refined using a riding model (Figure 2). Although there are no significant changes to the arrangement of the $[\text{BARF}_4]^-$ anions, this

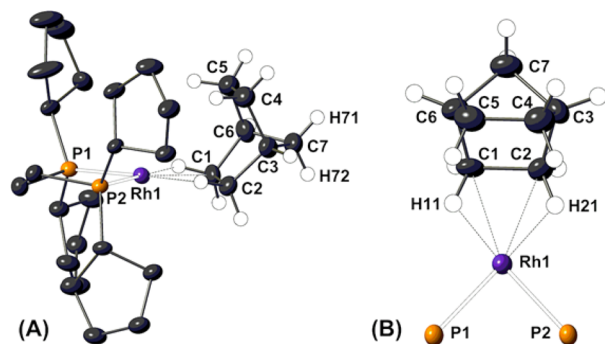


Figure 2. (A) Solid-state structure of $[\text{3-NBA}][\text{BARF}_4]$, with the cation and selected H atoms shown (100 K, 50% displacement ellipsoids). (B) Alternate view of $[\text{3-NBA}][\text{BARF}_4]$, with P-alkyl groups removed. Selected bond lengths (Å): $\text{Rh1}-\text{C1}$ 2.388(5), $\text{Rh1}-\text{C2}$ 2.392(5), $\text{Rh1}-\text{P1}$ 2.207(1), $\text{Rh1}-\text{P2}$ 2.206(1), $\text{C1}-\text{C2}$ 1.550(7), $\text{C4}-\text{C5}$ 1.541(9). Computed bond lengths (Å; periodic DFT, PBE-D3): $\text{Rh1}-\text{C1}$ 2.425, $\text{Rh1}-\text{C2}$ 2.420, $\text{Rh1}-\text{P1}$ 2.219, $\text{Rh1}-\text{P2}$ 2.215, $\text{C1}-\text{C2}$ 1.561, $\text{C4}-\text{C5}$ 1.565, $\text{Rh1}\cdots\text{H11}$ 1.895, $\text{Rh1}\cdots\text{H21}$ 1.886, $\text{C1}-\text{H11}$ 1.154, $\text{C2}-\text{H21}$ 1.154.

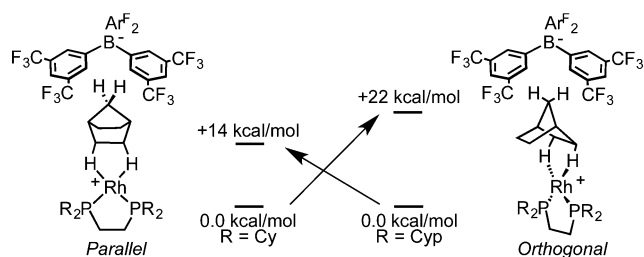
transformation proceeds with loss of the crystallographically imposed C_2 rotational symmetry: $[\text{3-NBD}][\text{BARF}_4]$, C_2/c , $Z = 4$; $[\text{3-NBA}][\text{BARF}_4]$, $P2_1/c$, $Z = 4$.¹⁰ Space group changes have been noted in other single-crystal transformations.^{5,11} The alkane ligand binds to the $\{\text{Rh}(\text{L}_2)\}^+$ fragment through two C–H σ -interactions, resulting in a Rh(I) square-planar, d^8 metal center coordination motif. The Rh–C1/C2 distances (2.388(5) and 2.392(5) Å, respectively) are the same, within error, as for $[\text{2-NBA}][\text{BARF}_4]$ (2.389(3) and 2.400(3) Å). The C1–C2 and C4–C5 distances (1.550(7) and 1.541(9) Å) signal the hydrogenation of the diene to form C–C bonds. The Rh–P distances (2.207(1) and 2.206(1) Å) are shorter than those in $[\text{3-NBD}][\text{BARF}_4]$ (2.2712(12) Å), reflecting the weaker trans influence C–H σ interactions. The Cyp groups showed some disorder.

The changes upon hydrogenation were also probed by the optimization of the extended solid-state structure with periodic DFT calculations at the PBE-D3 level. These provided excellent agreement both for the molecular geometries of the Rh cations (see the caption of Figure 2 for $[\text{3-NBA}][\text{BARF}_4]$ and the Supporting Information for $[\text{3-NBD}][\text{BARF}_4]$) and for the extended structure (see Figure S15 in the Supporting Information). Moreover, the calculations provide further insight into the $\text{Rh}\cdots\text{alkane}$ interaction, with short average computed $\text{Rh}\cdots\text{H11}/\text{H21}$ distances (1.89 Å) and elongated C1–H11 and C2–H21 distances (1.15 Å). In contrast, the C1–H12 and C2–H22 bonds exhibit standard distances of 1.10 Å, consistent with an absence of any interaction with Rh in that case. The $\text{Rh}\cdots\text{H}-\text{C}$ σ -interaction is confirmed by a quantum theory of atoms in molecules (QTAIM) study that identifies $\text{Rh}\cdots\text{H11}$ and $\text{Rh}\cdots\text{H21}$ bond paths with reduced electron densities for the C1–H11 and C2–H21 bond critical points in comparison to the C1–H12 and C2–H22 bonds.⁹

Consideration of the relationship between the cation and the proximal capping $[\text{BARF}_4]^-$ anion (Figure 1) shows that the NBA ligand in $[\text{3-NBA}][\text{BARF}_4]$ adopts an orientation very similar to that of the NBD ligand in $[\text{3-NBD}][\text{BARF}_4]$, in particular the orientation of the C7-methylene protons that are still directed toward the aryl rings. In contrast the $\{\text{Rh}(\text{L}_2)\}^+$ fragment has undergone a ca. 90° twist with respect to the precursor as defined by, for example, the interplane angle $\text{C38}, \text{C54}, \text{Rh1}/\text{Rh1}, \text{P1}, \text{P2} = 88.12(12)^\circ$ (Figure 1). We have previously noted¹² that the octahedral cavity described by the anions accommodates a variety of structural changes associated at the metal cation. Clearly it can also accommodate significant movement of the $\{\text{Rh}(\text{L}_2)\}^+$ fragment. Whether this occurs in concert with hydrogenation, or immediately afterward, is opaque to experiment. This situation is different from that observed in the transformations that afforded $[\text{2-NBA}][\text{BARF}_4]$, in which it is the organic fragment that responds by moving rather than $\{\text{Rh}(\text{L}_2)\}^+$.⁵ Isomerization, or dynamic processes, in single-crystal organometallics have been reported.¹³

Computationally the alternative form of $[\text{3-NBA}][\text{BARF}_4]$ was probed by rotating one complete cation within the unit cell and reoptimizing the structure (Scheme 2). This gives a local “parallel” structure analogous to that seen within $[\text{2-NBA}][\text{BARF}_4]$ and equivalent to the structure that would be formed if, upon hydrogenation, the NBD ligand in $[\text{3-NBD}][\text{BARF}_4]$ underwent rotation rather than the $\{\text{Rh}(\text{L}_2)\}^+$ cation. For $[\text{3-NBA}][\text{BARF}_4]$ the parallel structure is ca. 14 kcal/mol above the optimized “orthogonal” form. The parallel structure is therefore not viable thermodynamically, but it may be kinetically accessible, 14 kcal/mol representing a lower limit to the

Scheme 2. Relative Energies for Parallel and Orthogonal Forms



rearrangement barrier. For the more rigid [2-NBA][BARF₄] the experimentally observed⁵ parallel structure lies 22 kcal/mol below the alternative orthogonal form.

The hydrogenation of microcrystalline [3-NBD][BARF₄] was studied by SSNMR. A ³¹P{¹H} SSNMR spectrum (298 K) taken immediately after H₂ addition (10 min) shows complete consumption of [3-NBD][BARF₄], with two overlapping doublet signals observed (δ 109.2, $J_{\text{RhP}} \approx 189$ Hz; δ 108.1, $J_{\text{RhP}} \approx 188$ Hz), consistent with at least two crystallographically independent ³¹P environments. Such a downfield shift and increase in the J_{RhP} value are consistent with the formation of a σ -alkane complex.^{4,5,14} The ¹³C{¹H} SSNMR spectrum lacks signals between δ 100 and 50 due to NBD.⁹ We,^{5,14} and others,¹⁵ have previously used HETCOR SSNMR experiments to indirectly detect ¹H NMR signals in σ complexes, which in combination with computed chemical shifts has led to assignment of signals arising from σ -Rh...H-C interactions in σ -alkane complexes. The projected ¹H NMR spectrum from the ¹³C/¹H FSLG-HETCOR SSNMR experiment conducted on freshly prepared [3-NBA][BARF₄] showed a broad high-field signal centered at ca. δ -1.46 which correlates to a partially obscured ¹³C signal at δ 25.⁹ These chemical shifts are comparable to those reported for the σ -Rh...H-C interactions in [2-NBA][BARF₄].⁵ An additional high-field signal at $\delta(^1\text{H})$ -0.16 (cross peak $\delta(^{13}\text{C})$ 40.5) is assigned to the ring-current-affected methylene bridge (C7) protons. A similar cross peak is observed for [3-NBD][BARF₄] ($\delta(^1\text{H})$ -1.74/ $\delta(^{13}\text{C})$ 69.3) in line with a similar orientation of the NBD ligand in the precursor.

Assignment of these NMR data on the basis of the computed ¹³C and ¹H chemical shifts for [3-NBA][BARF₄] derived from the full extended solid-state structure (GIPAW method, PBE functional) is shown in Figure 3. Those for C1 and C2 (δ^{calc} ca.

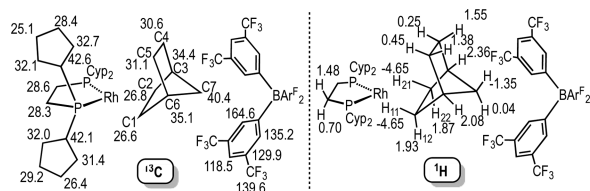


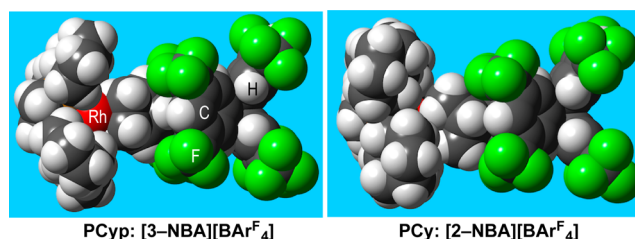
Figure 3. Computed ¹³C and ¹H chemical shifts for [3-NBA][BARF₄] (GIPAW, PBE functional).

27) are in good agreement with experiment, while the associated H11 and H21 exhibit appreciable shielding (coincident at δ^{calc} -4.65) but are shifted more upfield than those in experiment (δ -1.46). The C7 position (δ^{calc} 40.4) matches experiment, and the ring current effect that shields the C7 hydrogens is also captured. The different values for H71

and H72 (δ^{calc} -1.35 and 0.04) reflect the asymmetry of the environment in the static structure. The observation experimentally of single resonances for H71/72 (δ -0.16) and H11/21 may therefore reflect a fluxional process occurring on the NMR time scale at 298 K that renders these sets of protons equivalent. Cooling to 158 K resulted in a broadened ³¹P{¹H} SSNMR spectrum and a HETCOR in which signals due to the NBA ligand were too broad to be observed, consistent with a low-energy (~ 7 kcal/mol) fluxional process occurring in the solid-state.¹⁶ SSNMR calculations also reproduce well the change in J_{RhP} upon hydrogenation.⁹

Powdered crystalline [3-NBA][BARF₄] displayed stability intermediate between those of [1-NBA][BARF₄] (minutes) and [2-NBA][BARF₄] (months), as measured by ³¹P{¹H} SSNMR spectroscopy. Signals for [3-NBA][BARF₄] were slowly (96 h) replaced by a broad signal centered at δ 84, assigned to zwitterionic [3-BARF₄], as confirmed by an independent synthesis.⁹ Decomposition is effectively halted at 273 K.

Although we currently do not have a definitive explanation for the factors that control relative stabilities and the movements of NBA versus the metal fragment in the solid state, it may be noteworthy that the PCy₂ groups offer a more curved exterior surface in comparison with the rigid/tall PCy₂ that could encourage {Rh(L₂)}⁺ movement for the former in the relatively high symmetry cavity of [BARF₄]⁻ anions (Figure 4). The delineation of such electronic and steric influences will



Notes

The authors declare no competing financial interest.

■ ACKNOWLEDGMENTS

We acknowledge the EPSRC (A.S.W., S.A.M.; EP/M024210, EP/K035908, EP/K035681) for funding and Dr. Adrian Chaplin (University of Warwick) for useful discussions. This work used the ARCHER UK National Supercomputing Service (<http://www.archer.ac.uk>).

■ REFERENCES

- (1) (a) Hall, C.; Perutz, R. N. *Chem. Rev.* **1996**, *96*, 3125–3146. (b) Labinger, J. A.; Bercaw, J. E. *Nature* **2002**, *417*, 507–514. (c) Jones, W. D. *Acc. Chem. Res.* **2003**, *36*, 140–146. (d) Young, R. D. *Chem. - Eur. J.* **2014**, *20*, 12704–12718.
- (2) (a) McNamara, B. K.; Yeston, J. S.; Bergman, R. G.; Moore, C. B. *J. Am. Chem. Soc.* **1999**, *121*, 6437–6443. (b) Bernskoetter, W. H.; Schauer, C. K.; Goldberg, K. I.; Brookhart, M. *Science* **2009**, *326*, 553–556. (c) Torres, O.; Calladine, J. A.; Duckett, S. B.; George, M. W.; Perutz, R. N. *Chem. Sci.* **2015**, *6*, 418–424. (d) Yau, H. M.; McKay, A. I.; Hesse, H.; Xu, R.; He, M.; Holt, C. E.; Ball, G. E. *J. Am. Chem. Soc.* **2016**, *138*, 281–288.
- (3) Pike, S. D.; Weller, A. S. *Philos. Trans. R. Soc., A* **2015**, *373*, 20140187.
- (4) Pike, S. D.; Thompson, A. L.; Algarra, A. G.; Apperley, D. C.; Macgregor, S. A.; Weller, A. S. *Science* **2012**, *337*, 1648–1651.
- (5) Pike, S. D.; Chadwick, F. M.; Rees, N. H.; Scott, M. P.; Weller, A. S.; Krämer, T.; Macgregor, S. A. *J. Am. Chem. Soc.* **2015**, *137*, 820–833.
- (6) (a) Grellier, M.; Mason, S. A.; Albinati, A.; Capelli, S. C.; Rizzato, S.; Bijani, C.; Coppel, Y.; Sabo-Etienne, S. *Inorg. Chem.* **2013**, *52*, 7329–7337. (b) Douglas, T. M.; Brayshaw, S. K.; Dallanegra, R.; Kociok-Köhne, G.; Macgregor, S. A.; Moxham, G. L.; Weller, A. S.; Wondimagegn, T.; Vadivelu, P. *Chem. - Eur. J.* **2008**, *14*, 1004–1022. (c) Hackett, M.; Ibers, J. A.; Whitesides, G. M. *J. Am. Chem. Soc.* **1988**, *110*, 1436–1448.
- (7) Betteridge, P. W.; Carruthers, J. R.; Cooper, R. I.; Prout, K.; Watkin, D. J. *J. Appl. Crystallogr.* **2003**, *36*, 1487.
- (8) Wagner, T.; Schönleber, A. *Acta Crystallogr., Sect. B: Struct. Sci.* **2009**, *65*, 249–268.
- (9) See the [Supporting Information](#).
- (10) Initial data collection at 150 K revealed a poorer structure with significantly larger displacement ellipsoids associated with the NBA. There is only a 0.9% change in unit cell volume between [3-NBD][BAr^F₄] and [3-NBA][BAr^F₄] at 150 K: $V = 6142.10(16)$, $6197.3(3)$ Å³, respectively.
- (11) Lim, S. H.; Olmstead, M. M.; Balch, A. L. *Chem. Sci.* **2013**, *4*, 311–318.
- (12) Pike, S. D.; Krämer, T.; Rees, N. H.; Macgregor, S. A.; Weller, A. S. *Organometallics* **2015**, *34*, 1487–1497.
- (13) (a) Bogadi, R. S.; Levendis, D. C.; Coville, N. J. *J. Am. Chem. Soc.* **2002**, *124*, 1104–1110. (b) Edwards, A. J.; Burke, N. J.; Dobson, C. M.; Prout, K.; Heyes, S. J. *J. Am. Chem. Soc.* **1995**, *117*, 4637–4653.
- (14) Chadwick, F. M.; Rees, N. H.; Weller, A. S.; Krämer, T.; Iannuzzi, M.; Macgregor, S. A. *Angew. Chem., Int. Ed.* **2016**, *55*, 3677–3681.
- (15) Smart, K. A.; Grellier, M.; Coppel, Y.; Vendier, L.; Mason, S. A.; Capelli, S. C.; Albinati, A.; Montiel-Palma, V.; Munoz-Hernandez, M. A.; Sabo-Etienne, S. *Inorg. Chem.* **2014**, *53*, 1156–1165.
- (16) Chadwick, F. M.; Krämer, T.; Gutmann, T.; Rees, N. H.; Thompson, A. L.; Edwards, A. J.; Buntkowsky, G.; Macgregor, S. A.; Weller, A. S. *J. Am. Chem. Soc.* **2016**, DOI: [10.1021/jacs.6b07968](https://doi.org/10.1021/jacs.6b07968).